Journal of Molecular Graphics and Modelling 46 (2013) 1–9

Contents lists available at ScienceDirect

Journal of Molecular Graphics and Modelling

journal homepage: www.elsevier.com/locate/JMGM

Multi-conformation dynamic pharmacophore modeling of the peroxisome proliferator-activated receptor γ for the discovery of novel agonists

Young-sik Sohn[a], Chanin Park[a], Yuno Lee[a], Songmi Kim[a], Sundarapandian Thangapandian[a], Yongseong Kim[a,b], Hyong-Ha Kim[a,c], Jung-Keun Suh[a,d], Keun Woo Lee[a,*]

[a] Division of Applied Life Science (BK21 Program), Systems and Synthetic Agrobiotech Center (SSAC), Plant Molecular Biology and Biotechnology Research Center (PMBBRC), Research Institute of Natural Science (RINS), Gyeongsang National University (GNU), 501 Jinju-daero, Gazha-dong, Jinju 660-701, Republic of Korea
[b] Department of Science Education, Kyungnam University, Masan 631-701, Republic of Korea
[c] Division of Quality of Life, Korea Research Institute of Standards and Science, Daejeon 305-340, Republic of Korea
[d] Bio Computing Major, Korean German Institute of Technology, Seoul 157-033, Republic of Korea

ARTICLE INFO

Article history:
Received 25 March 2013
Received in revised form 9 August 2013
Accepted 12 August 2013
Available online 22 August 2013

Keywords:
Peroxisome proliferator-activated receptor γ
Multi-conformation dynamic pharmacophore modeling
Molecular dynamics simulation
Drug design
Type 2 diabetes

ABSTRACT

Activation of the peroxisome proliferator-activated receptor γ (PPARγ) is important for the treatment of type 2 diabetes and obesity through the regulation of glucose metabolism and fatty acid accumulation. Hence, the discovery of novel PPARγ agonists is necessary to overcome these diseases. In this study, a newly developed approach, multi-conformation dynamic pharmacophore modeling (MCDPM), was used for screening candidate compounds that can properly bind PPARγ. Highly populated structures obtained from molecular dynamics (MD) simulations were selected by clustering analysis. Based on these structures, pharmacophore models were generated from the ligand-binding pocket and then validated to check the rationality. Consequently, two hits were retrieved as final candidates by utilizing virtual screening and molecular docking simulations. These compounds can be used in the design of novel PPARγ agonists.

1. Introduction

The peroxisome proliferator-activated receptor γ (PPARγ) is a member of the nuclear receptor superfamily. PPARγ is mainly expressed in adipose tissue and regulates gene expression during transcription. The receptor operates with retinoid X receptor (RXR) to enhance binding at defined nucleotide sequences containing direct repeats of a hexanucleotide sequence in the 5′-flanking sequence of peroxisome proliferator inducible genes (peroxisome proliferator response element, PPRE) [1–4]. The PPARγ–RXR complex recognizes a variety of ligand types due to a large pocket around the C-terminal region of PPARγ. This large pocket contains six hydrophilic residues Gln286, Ser289, His323, Tyr327, His449, and Tyr473 [5]. Ligand binding results in the release of a corepressor and the recruitment of a coactivator, that, in turn, regulates basal transcription factors, which are necessary for transcription [6,7]. The structure of the complex includes PPARγ, RXR, ligands, PPRE, and coactivator peptides; the interaction between these components has been studied using X-ray crystallography to determine the mechanism of the formation of the protein complex [8]. PPARγ has seven different subtypes, depending on their expressed location. This receptor consists of four domains, namely, the DNA-binding domain (DBD), ligand-binding domain (LBD), transcription regulation domain, and hinge domain. The DBD binds to the AGGTCA sequence of PPRE, and the hinge domain forms an extensive interaction with DAN to reinforce DNA binding. The PPARγ–RXR complex contains three distinct heterodimerization surfaces formed by the DBD and the LBD. Notably, a surface residue of the ligand-binding pocket can affect domain–domain interactions and, ultimately, influence the DNA binding properties of the receptors. This interaction demonstrates that the LBD affects not only ligand binding but also the formation of the transcription complex. As they form an important functional domain, both the DBD and the LBD are linked by the hinge domain and are highly

* Corresponding author. Tel.: +82 55 772 1360; fax: +82 55 772 1359.
E-mail address: kwlee@gnu.ac.kr (K.W. Lee).

1093-3263/$ – see front matter © 2013 Published by Elsevier Inc.
http://dx.doi.org/10.1016/j.jmgm.2013.08.012

conserved. However, various lengths and sequences have been discovered in the other two domains of PPARγ [8–11].

Nuclear receptors typically have many target tissues; however, PPARγ is largely expressed in adipose tissue, the colon, vascular walls, and macrophages. The function of this protein is the stimulation of genes by acting as a transcription factor, such as how adipophilin or the liver fatty acid binding protein function in lipid transport and protein storage, respectively. In addition, many disease-related genes are induced by PPARγ, such as the cytokeratins associated proteins (differentiation related molecules), members of the carcinoembryonic antigen family (glycoproteins involved in adhesion), Drg-1 (a metastasis suppressor), and sialyltransferase (a glycosylation associated enzyme), among others. In contrast, other genes are repressed by PPARγ, such as cell cycle related factors containing cyclin D and protein phosphatase 2A, matrix metalloproteinase, the positive regulator of proliferation, and polyamine metabolizing enzyme (ornithine decarboxylase) [11].

Thiazolidinediones (TZDs), a drug family of PPARγ agonists, possess PPARγ-independent effects, which are destructive to other proteins. These compounds increase cyclin-dependent kinase (CDK) inhibitor p27 protein levels which arrest proteasomes, inhibit tumor angiogenesis induced by direct action on the vessel endothelial cells, and suppress cholesterol biosynthesis and glyconeogenesis. The naturally occurring PPARγ ligand, 15-deoxy-$\Delta^{12,14}$-PGJ_2 (15d-PGJ_2), possesses non-PPARγ-mediated activity. This compound activates the extracellular signal-regulated kinase, which in turn leads to apoptosis and G1 arrest [11]. While TZDs and non-TZDs, which have high affinity and full agonistic activity, including side effects, partial agonists consisting SR1664 and SR1824 do not show any adverse reaction, even as they lead to the recovery of glucose homeostasis. These compounds increase the conformational mobility of helix 11 (residues 439–459) but do not interact with helix 12 (residues 467–473). The interruption of phosphorylation that is mediated by CDK5 is a key element in the development of a new class of PPARγ agonists [8,12]. These studies indicate that novel class of agonists, which are not ligands with a classical agonistic activity, are considered important for the treatment of type 2 diabetes without side effects.

The main goal of this study was to select more effective PPARγ agonists using multi-conformation dynamic pharmacophore modeling (MCDPM). To consider the flexibility of the LBD, we have developed a new method, which performs receptor-based dynamic pharmacophore modeling (RDPM) with two different ligand-bound structures. The crystal structure of human PPARγ (PDB ID: 2ATH) was selected as an initial conformation for the molecular dynamics (MD) simulations [13]. The structures of two different ligands were used to perform the MD simulation, and three pharmacophore models were generated from each system. Thus, the pharmacophore models obtained from MCDPM will add another dimension for designing novel and potential PPARγ agonists.

2. Methods

2.1. Molecular dynamics simulations and the selection of representative structures

To obtain diverse conformations of PPARγ, two MD simulations were performed, using the *GROMACS 4.0* package [14,15], with the rosiglitazone bound system (PPARγ-R) and the NCI0077416 bound system (PPARγ-N). Rosiglitazone is an antidiabetic drug that functions as an agonist of PPARγ and NCI0077416 was discovered as a potential candidate, with PPARγ agonistic activity, from our previous study [16]. During the preparation procedure for the MD simulation, the ionizable residues of the protein were protonated without artifacts, and all of the information of the atoms was presented by topology files using the PRODRG server [17]. Then, neutralization of the system was achieved by the addition of 5 Na^+, and steepest descent energy minimization of the protein–ligand complex was performed in a water box of $39.84 \times 53.77 \times 61.44$ Å^3. The steepest descent energy minimization stabilizes the protein by removing possible bad contacts until the energy has converged below 2000 kJ/mol. Next, 100 ps position restrained MD simulations were performed and followed by 5 ns production MD simulations at a constant pressure (1 atm) and temperature (300 K). The PME algorithm for calculating electrostatic interactions and the SHAKE algorithm to fix all bonds were used [18]. The computational time step and the accumulation of coordinates were set to every 2 fs and 1 ps, respectively. Based on the root mean-square deviation (RMSD) comparison of each snapshot from the MD simulation, clusters were generated by controlling the cutoff value. The energy of each conformation was compared with the lowest energy within the trajectory considering the Boltzmann factor to estimate the relative possibility of conformations. Finally, the clusters were sorted by the number of snapshots, and the representative structures, which are closest to the average conformation, were selected from the top three clusters of each system [19].

2.2. Pharmacophore modeling and validation

Based on the representative structures, pharmacophore model features were generated by the rule-based automatic design of new substituents for an enzyme inhibitor leads (Ludi) interaction map [20,21]. Many features, including hydrogen bond acceptor (HBA), donor (HBD), and hydrophobic (HY) features, were generated depending on the properties of the residues. From the large ligand-binding pocket between helix 3 and the β turn of PPARγ, pharmacophore features were created based on the six key residues (Gln286, Ser289, His323, Tyr327, His449, and Tyr473) because these residues keep the ligand in its correct position and sort the compounds [22]. The important features representing the specificity of each conformation were selected using the feature mapping module in the *Discovery Studio 3.0 (DS 3.0)* program [23]. The duplicated features showing the same chemical property were clustered to present representative features. Overlapping features indicating different properties were deleted because these different traits cannot exist in the same place [24]. To validate the rationality of the pharmacophore models, ligands of other proteins were mapped on the models. The fit value, which indicates how well the compounds match the pharmacophore features, should be low for these ligands in the developed pharmacophore models to prove the reliability of the developed pharmacophore models for PPARγ agonists. Ligands of aldosterone synthase (CYP11B2) and cyclin-dependent kinase 4 (CDK4) were assembled to generate databases because the functions of CYP11B2 and CDK4 are very different from PPARγ. CYP11B2 is a cytochrome P450 enzyme that generates aldosterone and catalyze many reactions, including the synthesis of cholesterol, steroids, and other lipids, as well as drug metabolism [25]. CDK4 is important for cell cycle G1 phase progression and is responsible for the phosphorylation of the retinoblastoma gene product [26]. The compounds constituting the databases were collected from the Binding Database, which is an organized dictionary composed of relational data for describing binding measurements [27]. All of the ligands in the databases were mapped to the developed pharmacophore models, and the fit values indicating the quality of mapping between compounds and pharmacophore models were obtained.

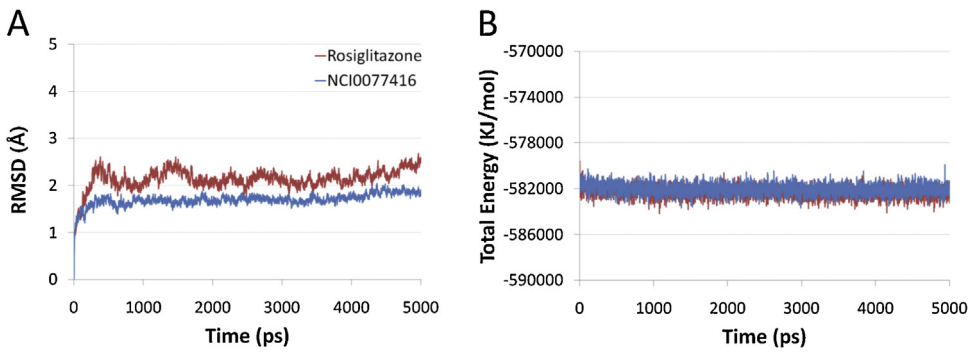

Fig. 1. The RMSD results of two ligand-bound (PPARγ-R and PPARγ-N) systems during the 5 ns molecular dynamics simulations (A). The total energies of both systems were measured to confirm stability (B).

2.3. Screening databases and the selection of candidates

After the validation, pharmacophore models were used as the first standard for screening candidates from Maybridge and NCI databases. A maximum of 250 conformations were generated for each compound using the *Best Conformational Analysis* method and the *Poling Algorithm* [28–30] to consider all of the possible conformations. Then, the Log *P*, topological polar surface area (TPSA), Lipinski's rule, and the number of rotatable bonds were calculated using the *Molinspiration* toolkit for the hit compounds [31]. The Log *P* is considered as a measurement of molecular hydrophobicity, which affects many factors, such as bioavailability, hydrophobic drug–receptor interactions, absorption, metabolism, and toxicity. The TPSA is also a descriptor of drug absorption, which considers O- and N-centered polar fragments [32]. Lipinski's rule of five for measuring the solubility or permeability of molecules states that drug-like compounds have the four following properties [33]: (i) the Log *P* is ≤5, (ii) the molecular weight is ≤500, (iii) the number of H-bond acceptors is 10 or fewer and (iv) the number of H-bond donors is ≤5. In addition to Lipinski's rule, a ligand, which has <10 rotatable bonds, has a high probability to show good oral bioavailability [34]. The 11 hit compounds were screened from the databases through the previous standards and two leads were selected as final candidates using a molecular docking study. The prediction of the binding affinity and calculation of the binding free energy were performed using the *GOLD 4.1* program [35] and the *PyRx 0.8* program [36], respectively. Although *GOLD* is optimized for estimating the binding position of the ligand, the sum of external terms among the GoldScore can predict binding affinity. The *PyRx*, using AutoDock, computes free energy by calculating a system's intermolecular, total internal, torsional, and unbound energy values. The values from these calculations were ranked, and the compounds with better results than rosiglitazone were selected as final hit compounds.

2.4. MD simulation study to validate the final hits

We performed MD simulations to compare rosiglitazone and the hit compounds by measuring energies and observing the interactions between PPARγ and the ligands. The same procedure and parameters used in simulating the protein–ligand complexes for cluster analyses were used in the simulations of hit compounds. After the RMSD was measured to observe the stability of proteins with final leads, the number of hydrogen bonds and their distances were monitored to compare interactions between final hits and PPARγ. Finally, a series of energy terms, including short-range Coulomb energy (Coul-SR), short-range Lennard–Jones potential energy (LJ-SR), and long-range Lennard–Jones potential energy (LJ-LR), were estimated to confirm the stability of the non-bonded interactions between the proteins and the final candidates. The Coulomb energy associates electrons of a covalent bond and is the standard of electrostatic forces within the system. The Lennard–Jones potential is a mathematical model which estimates the interactions of nonbonding atoms or molecules based on their distance of separation [37].

3. Results and discussion

3.1. MD simulations and clustering analysis

To obtain multiple conformations of the protein structure, 5 ns MD simulations were performed for two ligand-bound systems, including rosiglitazone and NCI0077416. First, the RMSD and total energy of the systems were calculated to check the system's stability (Fig. 1). The RMSD values for the both systems were maintained at <3 Å during the simulation time. Total energy plots for both the systems showed very stable behavior during the simulation time. These results indicated that the simulations performed well during the simulation times; there were no noticeable problems or artifacts.

Clustering analysis was carried out over the snapshots obtained from a 5 ns MD simulation based on the RMSDs of Cα atom positions. Each conformation was distributed to the same cluster when the distance to any group component was less than the fixed cut-off. In the PPARγ-R system, 10 clusters were generated with cut-off values of 0.635 Å (Fig. 2A), and the top three clusters accounted for 74.61% of the total. The snapshots at 3552 ns, 2518 ns, and 1126 ns were selected as the nearest to the average structures from cluster 1, cluster 2, and cluster 3, respectively. All of the six key residues of the snapshots displayed different conformations (Fig. 2C). All the snapshots of the PPARγ-N system were divided by 12 clusters with a cut-off value of 0.638 Å (Fig. 2B). From the top three clusters which occupy 58.25% of the total, the closest structures were at 4358 ns (cluster 1), 2932 ns (cluster 2), and 3694 ns (cluster 3) to the average structure; these structures were selected as representative. At the LBD, the Gln286 and Tyr473 residues showed differences in their conformations (Fig. 2D). By using these structures, different conformations of PPARγ were considered for the generation of the pharmacophore models for the database screening.

3.2. Generation and validation of pharmacophore models

The knowledge of protein–ligand interactions and the availability of the 3D structure are required for the generation of a dynamic pharmacophore model [38]. Accordingly, the representative structures were selected from the clustering analysis of the MD simulation snapshots. From each representative structure, numerous chemical features, including the HBA, HBD, and HY

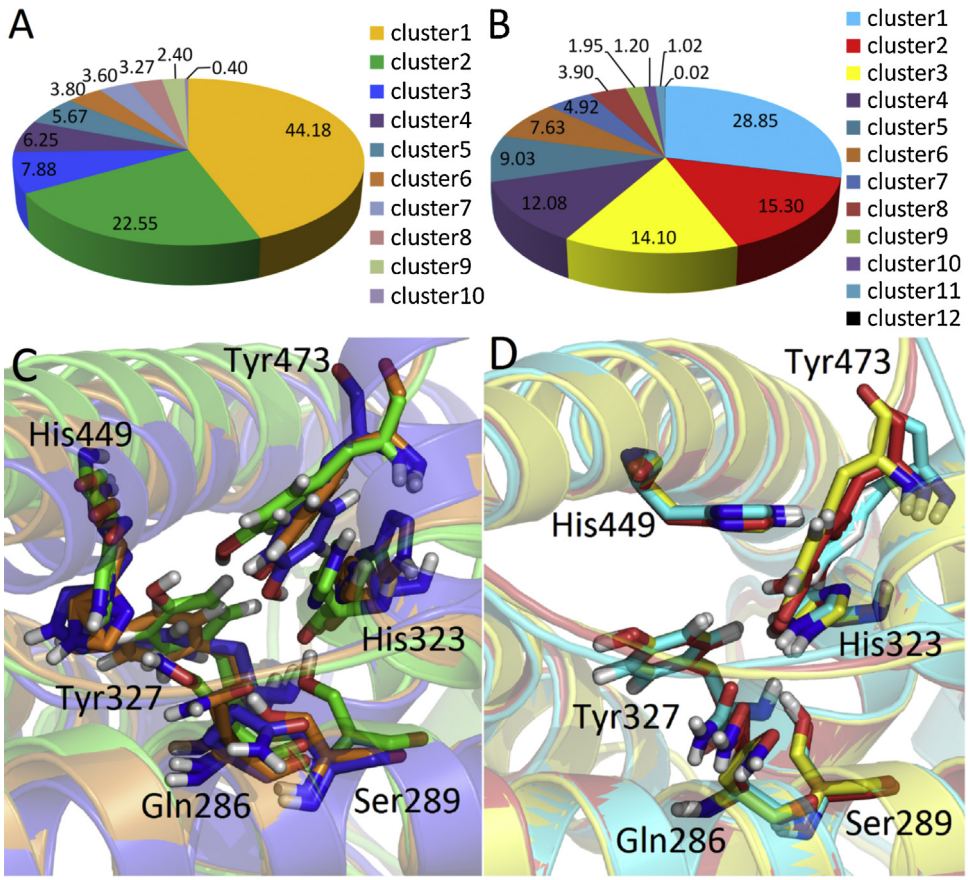

Fig. 2. Clustering results and representative structures. Ten clusters and twelve clusters were generated from the PPARγ-R (A) and PPARγ-N (B) systems, respectively. Representative structures of the top three clusters, (C) PPARγ-R and (D) PPARγ-N, were superimposed.

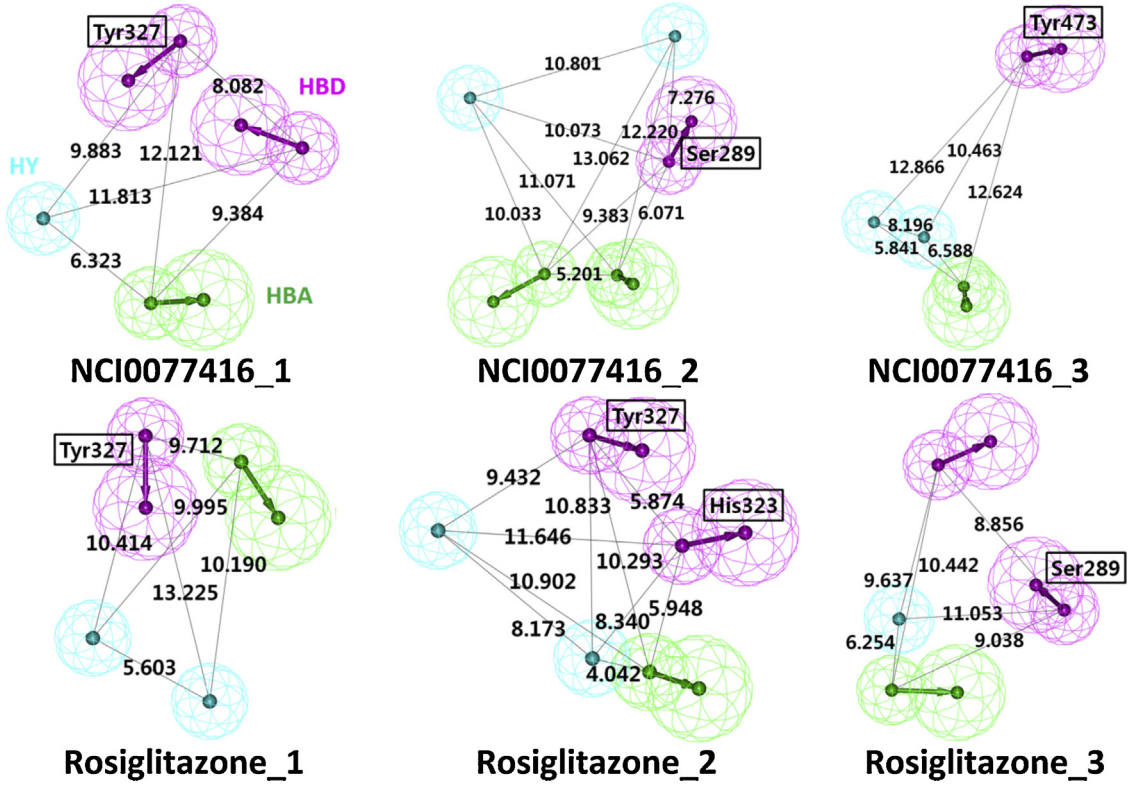

Fig. 3. The 3D representation of the developed pharmacophore models, including inter-feature distances denoted in Å units. All of the models contain hydrogen bond acceptors (HBA, green), hydrogen-bond donors (HBD, magenta), and hydrophobic (HY, blue) features. The key amino acid residues of the LBD are labeled. (For interpretation of the references to color in this figure legend, the reader is referred to the web version of this article.)

Table 1
Validation of pharmacophore models by mapping agonists on six models.

Pharmacophore model	Fit value		PPARγ(193)[a]		CYP11B2(279)[a]		CDK4(200)[a]	
	Rosiglitazone	NCI0077416	Fitted ligand	Fit value[b]	Fitted ligand	Fit value	Fitted ligand	Fit value[b]
NCI0077416_1	2.1956	2.5535	162	1.6955	0	0	1	0.3655
NCI0077416_2	2.9247	2.9784	193	2.6954	0	0	0	0
NCI0077416_3	2.9642	2.9981	192	2.9129	0	0	1	0.4490
Rosiglitazone_1	2.9567	2.9979	189	2.6871	0	0	7	1.1753
Rosiglitazone_2	2.9937	3.4279	193	2.9372	0	0	0	0
Rosiglitazone_3	2.6511	2.8405	193	1.9829	0	0	1	0.7361

[a] The number in the parenthesis indicates the amount of compounds of the protein.
[b] The average cost of fit values.

features, were generated based on the key residues of the ligand-binding pocket. Six pharmacophore models (NCI0077416_1, 2, 3 and Rosiglitazone_1, 2, 3) generated from the representative structures were developed with four or five chemical features because four or five point models effectively retrieve hits from databases [19]. All of the pharmacophore models revealed diverse 3D locations, indicating that the models were able to screen ligands bind the multi-conformational structure of PPARγ (Fig. 3). To verify the quality of the pharmacophore models, fit values were compared between known agonists and ligands of other proteins (Table 1). All of the calculated fit values of rosiglitazone and NCI0077416 were over 2.5, except for one; the highest fit value was 3.4279. The 193 known agonists of PPARγ from an in-house database also support the finding that the pharmacophore models can screen for appropriate candidates. However, the 279 ligands of CYP11B2 did not fit any of the pharmacophore models and the CDK4 ligands did not fit well in any of the models. These results indicated that all the generated pharmacophore models could be specifically used in filtering PPARγ agonists more from the chemical databases.

3.3. Virtual screening and the selection of final candidates

As the first step of virtual screening, six validated pharmacophore models were used for search queries to retrieve PPARγ agonists from the chemical databases (Maybridge and NCI). Each model effectively filtered chemical compounds, which fit well on the pharmacophore models and reduced the number ligands by over 90% from the databases. After the leads were screened by Lipinski's rule and fit value, 10 common chemical compounds from the NCI database and 1 hit compound from the Maybridge database were obtained (Fig. 4). For verification, we compared the degree of matching between hit compounds and inactive compounds on the pharmacophore models. The selected inactive compound was clofibrate that had an EC_{50} value >500,000 nM [39]. Clofibrate mapped with only two chemical features of each pharmacophore model, but the hit compounds mapped with all of the models, especially the features related to the key residue (Fig. 5). This result indicated that the 11 hit compounds demonstrated the potential to act as powerful agonists of PPARγ.

From these 11 hits, final candidates were selected based on the molecular docking results and fit values. First, the estimated free energy and GoldScore of the hit compounds were calculated and ranked (Table 2). In the table, GoldScore indicates the sum of S(hb_ext) and $1.375 \times$ S(vdw_ext) for predicting binding affinity [35]. The appropriateness of the hit compounds was confirmed by the estimation and comparison of the values of rosiglitazone. HTS08858 from the Maybridge database was chosen as the best-hit compound because it showed the lowest energy value and a comparatively high GoldScore. Second, we observed the fit values between each pharmacophore model and the candidates. NCI0112919, NCI0135516, and NCI0107490 showed the best-fit values in three models (NCI0077416_2, Rosiglitazone_1 and 2), two models (NCI0077416_1 and Rosiglitazone_3), and one model (NCI0077416_3), respectively (Table 3). Based on these results, NCI0135516 was also selected as a final candidate. Although NCI0135516 had a high energy value compared with the other hit compounds, it presented the highest GoldScore and the highest fit value in two pharmacophore models.

Table 2
Molecular docking simulation results.

Hit compound	Estimated free energy (kcal/mol)	GoldScore[a]	Rank
HTS08858	−7.30	77.59	1
NCI0107490	−7.25	74.73	2
NCI0135516	−5.72	79.99	3
NCI0130220	−7.03	72.00	4
Rosiglitazone	−7.18	70.96	4
NCI0103834	−3.59	79.99	6
NCI0112919	−6.98	69.13	6
NCI0106148	−4.46	78.31	8
NCI0131547	−6.24	62.21	9
NCI0129807	−5.08	67.45	10
NCI0036404	−6.03	48.30	11
NCI0050131	−4.78	62.02	12

[a] The cost is the sum of external term score which means prediction of binding affinity.

3.4. Validation of hit compounds using MD simulations

The 2D structures of the final hit compounds are different from rosiglitazone in terms of their chemical structure (Fig. 6A). To confirm their potential as PPARγ agonists, 5 ns MD simulations of the enzyme-hit compound complexes were performed. The RMSD and the number of hydrogen bonds were calculated to confirm the stability of the proteins and the maintenance of interactions between ligands and key residues (Fig. 6B and C). These systems were stable during 5 ns, as observed from the RMSD result. However, the systems showed a difference in the number of hydrogen bond interactions. The PPARγ-HTS08858 and PPARγ-NCI0135516 systems formed more than two hydrogen bonds on average during the last 2 ns, but the PPARγ-R system showed less than two hydrogen bonds (Table 4). The distance between each hydrogen bond was measured. This allowed for the confirmation of the protein–ligand interactions of each system by the selection of representative structures (3552 ns (PPARγ-R), 3633 ns (PPARγ-HTS08858), and 3587 ns (PPARγ-NCI0135516)), which verified that

Table 3
Pharmacophore mapping result of the most fitted compound and fit value.

Pharmacophore model	Compound	Fit value
NCI0077416_1	NCI0135516	3.7943
NCI0077416_2	NCI0112919	3.7036
NCI0077416_3	NCI0107490	3.2130
Rosiglitazone_1	NCI0112919	2.9967
Rosiglitazone_2	NCI0112919	4.3569
Rosiglitazone_3	NCI0135516	3.4732

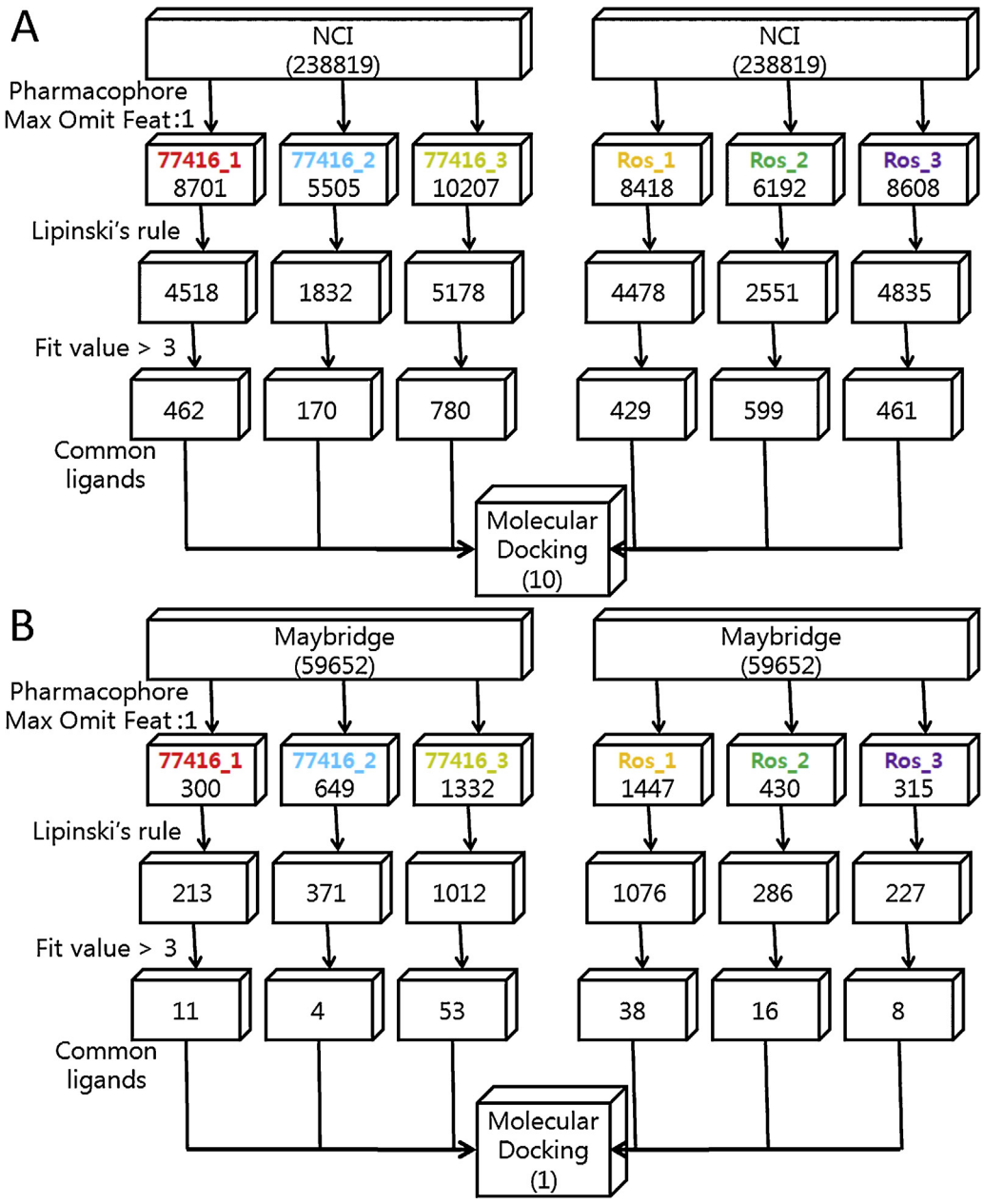

Fig. 4. Flowchart of the virtual screening process used in filtering the hit compounds from the NCI (A) and Maybridge databases (B).

the hit compounds could be novel agonists (Fig. 7). Although the distances of hydrogen bonds in PPARγ-NCI0135516 system were similar to the values of the PPARγ-R system, HTS08858 and the residues of PPARγ maintained a closer distance than the other systems (Table 4). In the PPARγ-R system, some oscillation in the hydrogen bond between Ser289-O25 and His449-O24 was observed, but the distance between Tyr473 and O24 was maintained at approximately 6 Å during the MD simulation (Fig. 7A). Initially, the distance between His449 and O16 of HTS08858 rose until it reached 8 Å; however, the distance eventually stabilized at 5 Å. The distance between Ser289-O9 and Tyr327-O23 was well maintained in the PPARγ-HTS08858 system (Fig. 7B). During the simulation, the distances of Ser289-O34, Tyr327-O1, and Tyr473-O33 in PPARγ-NCI0135516 system were

Table 4
PPARγ-ligand interaction information.

Hit compound	No. of H-bond[a]	Distance of H-bond (nm)[a]				Protein–ligand interactions	
		Ser289	Tyr327	His449	Tyr473	H-bond	Hydrophobic contacts [b]
Rosiglitazone	1.88	0.45	–	0.61	0.58	S289, H449, Y473	I281, *F282*, *C285*, Q286, *L330*, V339, I341, F363, M364, L453
HTS08858	2.47	0.32	0.50	0.54	–	S289, Y327, H449	A233, *F282*, *C285*, Q286, R288, I326, M329, *L330*, I341
NCI0135516	2.92	0.48	0.55	–	0.62	S289, Y327, Y473	I281, *F282*, *C285*, I326, *L330*, V339, M348, M364, F368, L453

[a] The value is the average cost of last 2 ns during MD simulation.
[b] Italicized residues formed hydrophobic contacts in common.

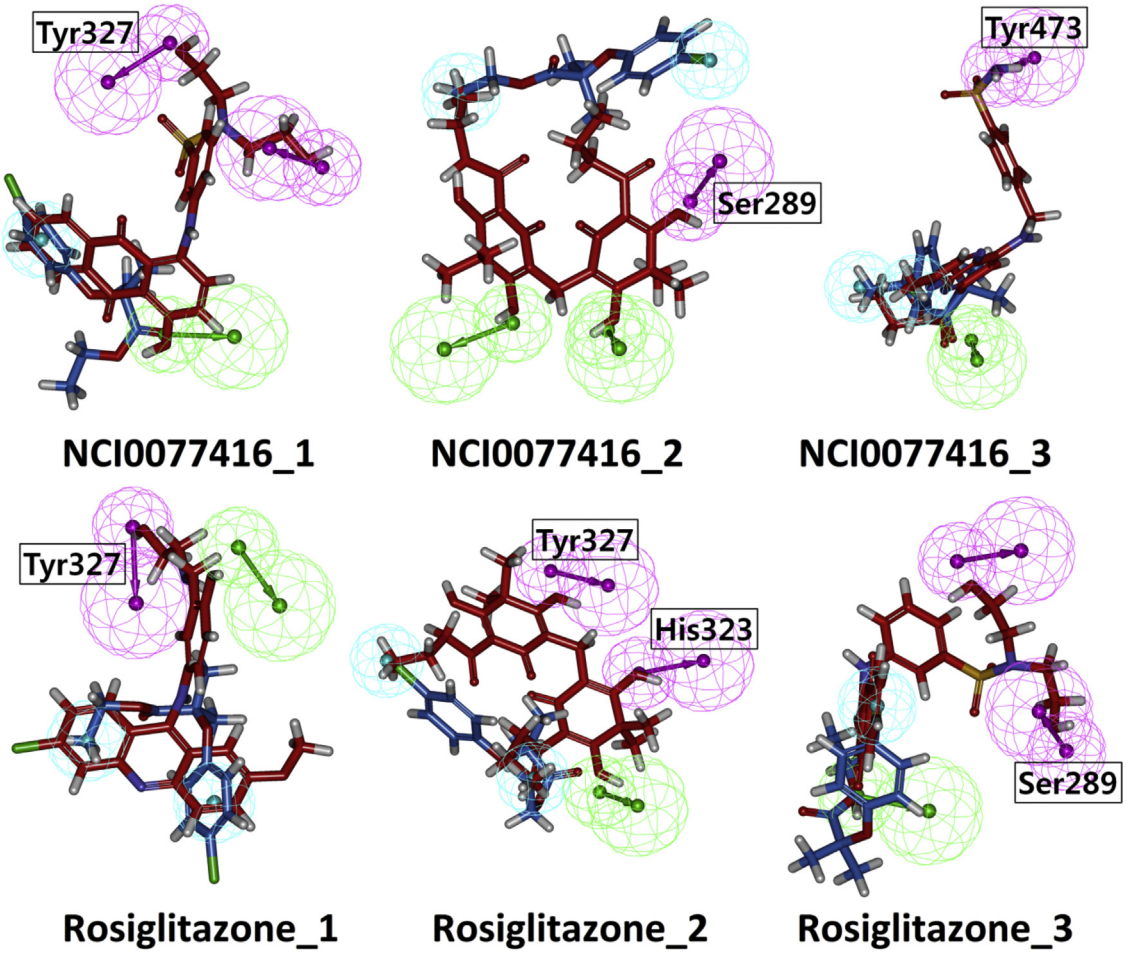

Fig. 5. Mapping results between pharmacophore models and compounds. Red colored ligands have the highest fit values and blue colored ligands have the lowest values (clofibrate, EC_{50} = 500,000 nM) in the generated pharmacophore models. (For interpretation of the references to color in this figure legend, the reader is referred to the web version of this article.)

approximately 5.0 Å, 5.5 Å, and 6.0 Å, respectively (Fig. 7C). From this result, it was observed that NCI0135516 had formed hydrogen bonds with key residues and formed the most favorable conformation among the three ligands. Additionally, the Phe282, Cys285, and Leu330 residues would be important for their interaction with the small molecule, which bound to PPARγ because these residues formed hydrophobic contacts with rosiglitazone and the hit compounds (Table 4). Finally, interaction energies were calculated and compared with each system to support the appropriateness of the hit compounds. In the LJ-SR and LJ-LR results, which indicate the van der Waals energy, the PPARγ-R system had a slightly higher value than the other systems (Fig. 8A and B). Nonetheless, the Coul-SR result, which is the standard for covalent bonds and electrostatic interactions, described a definite difference between the identified hits and rosiglitazone (Fig. 8C). The average costs of the energies during last 2 ns represented the correct gap between the known agonist and the hit compounds (Table 5). Two lead molecules, which showed better results compared to rosiglitazone, can be considered as powerful agonists targeting PPARγ.

3.5. MCDPM

Drug design using pharmacophore models can be divided into two categories, including ligand-based pharmacophore modeling

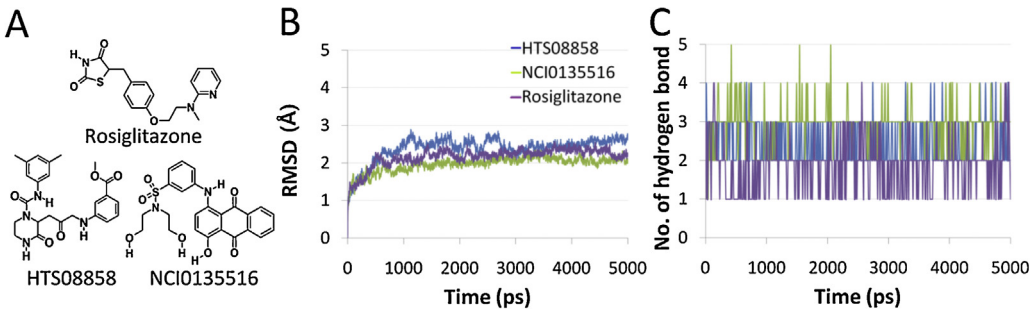

Fig. 6. The 2D structure comparison of rosiglitazone and hit compounds (A). The RMSD plots of three protein–ligand complexes (HTS08858, NCI0135516, and rosiglitazone) (B) and the number of hydrogen bonds formed by these ligands (C) during the 5 ns MD simulations.

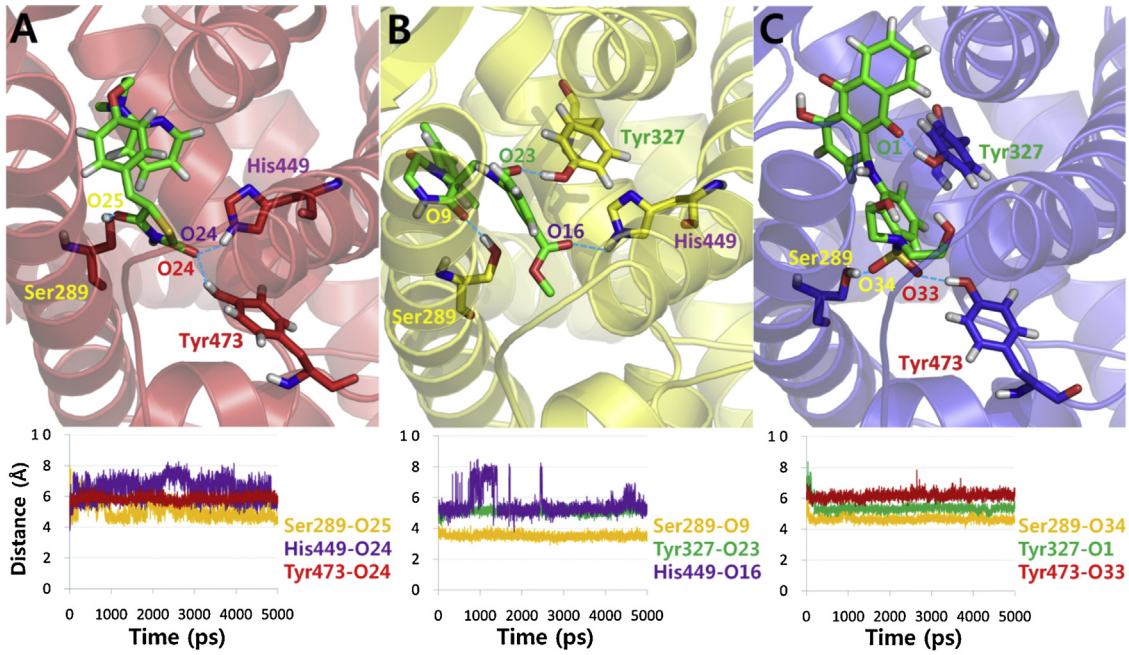

Fig. 7. Representative structures and hydrogen bond distances of PPARγ with the hit compounds throughout the simulation time: rosiglitazone (A), HTS08858 (B) and NCI0135516 (C). The perforated blue line indicates hydrogen bonds. (For interpretation of the references to color in this figure legend, the reader is referred to the web version of this article.)

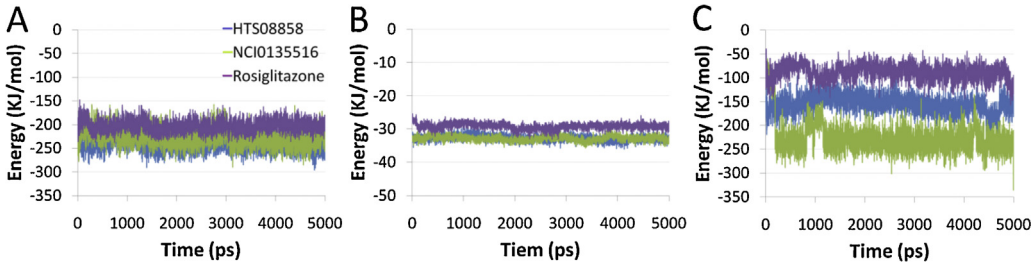

Fig. 8. Energy calculation results. The short-range Lennard–Jones potential (A), long-range Lennard–Jones potential (B), and Coulombic energy (C) for three complexes (HTS08858, NCI0135516, and rosiglitazone).

(LPM) and receptor-based pharmacophore modeling (RPM) methods. The LPM relies on information from molecules, which are experimentally known ligands of the target protein. The generated pharmacophore models are appropriate for screening candidates, which have similar properties to the known drugs. Nevertheless, the RPM utilizes the structural information of the target, especially the LBD. Thus, the pharmacophore model represents a 3D arrangement of the functional groups of the ligand-binding pocket. Receptor-based dynamic pharmacophore modeling (RDPM), a method based on the RPM, generates pharmacophore models using a series of representative conformations displayed by one ligand. The structural diversity obtained from a MD simulation is presented to several models [19]. Thus, the hit compounds using RDPM are able to bind to the protein for a long time. Yet, diverse conformations are able to emerge from different ligand-bound proteins. This is because the conformations of the binding pocket of the receptor are different, according to the ligand, even though the ligands have the same scaffold. A difference in activity among structurally similar compounds is also observed. This issue was kept in mind for the development of the MCDPM, which generates pharmacophore models using RDPM with different ligand-bound structures. In this study, this method was validated by the comparison of the MD simulation results between rosiglitazone and the hit compounds. In this respect, the MCDPM, which reflects many conformations of the protein, is able to play an important role in screening drug-like molecules.

Table 5
Average values of energies during last 2 ns.

Hit compound	LJ-SR (kcal/mol)	LJ-LR (kcal/mol)	Coul-SR (kcal/mol)
Rosiglitazone	−198.30	−29.36	−93.12
HTS08858	−222.35	−32.99	−163.31
NCI0135516	−223.91	−32.80	−232.87

4. Conclusion

In this study, the pharmacophore modeling method was utilized to design potent PPARγ agonists. MCDPM, a novel pharmacophore modeling method, was employed to consider multi-conformational aspects of the target protein. Six pharmacophore models were generated from ligand-binding site conformations, which were obtained from MD simulations. All of the models were composed of four or five chemical features, including HBA, HBD, and HY. These pharmacophore models were validated by their ability to identify active compounds and were utilized in virtual screening for the discovery of novel scaffolds. Structurally novel compounds were generated based on the models and drug-like filters. From the resulting hits, final candidates that showed better binding

compared to the existing drug were selected from the molecular docking simulation. Finally, MD simulations were performed to confirm the interactions between the protein and the final hit compounds. From these results, two compounds were selected as potent PPARγ agonists. The MCDPM method used in this study could be extended to other systems to identify drug-like molecules.

Acknowledgements

This research was supported by Basic Science Research Program (2012R1A1A4A01013657), Pioneer Research Center Program (2009-0081539), and Management of Climate Change Program (2010-0029084) through the National Research Foundation of Korea (NRF) funded by the Ministry of Education, Science and Technology (MEST) of Republic of Korea. And this work was also supported by the Next-Generation BioGreen 21 Program (PJ009486) from Rural Development Administration (RDA) of Republic of Korea.

References

[1] K.L. Gearing, M. Gottlicher, M. Teboul, E. Widmark, J.A. Gustafsson, Interaction of the peroxisome-proliferator-activated receptor and retinoid X receptor, Proc. Natl. Acad. Sci. U. S. A. 90 (1993) 1440–1444.
[2] I. Issemann, R. Prince, J. Tugwood, S. Green, The peroxisome proliferator-activated receptor: retinoid X receptor heterodimer is activated by fatty acids and fibrate hypolipidaemic drugs, J. Mol. Endocrinol. 11 (1993) 37.
[3] B. Desvergne, W. Wahli, Peroxisome proliferator-activated receptors: nuclear control of metabolism, Endocr. Rev. 20 (1999) 649–688.
[4] O. Bardot, T. Aldridge, N. Latruffe, S. Green, PPAR–RXR heterodimer activates a peroxisome proliferator response element upstream of the bifunctional enzyme gene, Biochem. Biophys. Res. Commun. 192 (1993) 37–45.
[5] K. Yamagishi, K. Yamamoto, Y. Mochizuki, T. Nakano, S. Yamada, H. Tokiwa, Flexible ligand recognition of peroxisome proliferator-activated receptor-γ (PPARγ), Bioorg. Med. Chem. Lett. 20 (2010) 3344–3347.
[6] J.N. Feige, L. Gelman, L. Michalik, B. Desvergne, W. Wahli, From molecular action to physiological outputs: peroxisome proliferator-activated receptors are nuclear receptors at the crossroads of key cellular functions, Prog. Lipid Res. 45 (2006) 120–159.
[7] M. Gurnell, Peroxisome proliferator-activated receptor γ and the regulation of adipocyte function: lessons from human genetic studies, Best Practice Res. Clin. Endocrinol. Metab. 19 (2005) 501–523.
[8] V. Chandra, P. Huang, Y. Hamuro, S. Raghuram, Y. Wang, T.P. Burris, F. Rastinejad, Structure of the intact PPAR-γ–RXR-α nuclear receptor complex on DNA, Nature 456 (2008) 350–356.
[9] Y. Chen, A.R. Jimenez, J.D. Medh, Identification and regulation of novel PPAR-γ splice variants in human THP-1 macrophages, Biochim. Biophys. Acta (BBA)-Gene Struct. Expr. 1759 (2006) 32–43.
[10] J.P. Renaud, D. Moras, Structural studies on nuclear receptors, Cell. Mol. Life Sci. 57 (2000) 1748–1769.
[11] I.A. Voutsadakis, Peroxisome proliferator-activated receptor γ (PPARγ) and colorectal carcinogenesis, J. Cancer Res. Clin. Oncol. 133 (2007) 917–928.
[12] J.H. Choi, A.S. Banks, T.M. Kamenecka, S.A. Busby, M.J. Chalmers, N. Kumar, D.S. Kuruvilla, Y. Shin, Y. He, J.B. Bruning, D.P. Marciano, M.D. Cameron, D. Laznik, M.J. Jurczak, S.C. Schürer, D. Vidović, G.I. Shulman, B.M. Spiegelman, P.R. Griffin, Antidiabetic actions of a non-agonist PPARγ ligand blocking Cdk5-mediated phosphorylation, Nature 477 (2011) 477–481.
[13] N. Mahindroo, C.F. Huang, Y.H. Peng, C.C. Wang, C.C. Liao, T.W. Lien, S.K. Chittimalla, W.J. Huang, C.H. Chai, E. Prakash, Novel indole-based peroxisome proliferator-activated receptor agonists: design, SAR, structural biology, and biological activities, J. Med. Chem. 48 (2005) 8194–8208.
[14] H. Berendsen, D. van der Spoel, R. van Drunen, GROMACS: a message-passing parallel molecular dynamics implementation, Comput. Phys. Commun. 91 (1995) 43–56.
[15] D. van der Spoel, E. Lindahl, B. Hess, A.R. van Buuren, E. Apol, P.J. Meulenhoff, et al., Gromacs User Manual version 4.0, 2005.
[16] Y. Sohn, Y. Lee, C. Park, S. Hwang, S. Kim, A. Baek, M. Son, J.K. Suh, H.H. Kim, K.W. Lee, Pharmacophore identification for peroxisome proliferator-activated receptor gamma agonists, Bull. Korean Chem. Soc. 32 (2011) 201–207.
[17] A.W. Schuttelkopf, D.M.F. Van Aalten, PRODRG: a tool for high-throughput crystallography of protein–ligand complexes, Acta Crystallogr., Sect D: Biol. Crystallogr. 60 (2004) 1355–1363.
[18] K. Bharatham, N. Bharatham, Y.J. Kwon, K.W. Lee, Molecular dynamics simulation study of PTP1B with allosteric inhibitor and its application in receptor based pharmacophore modeling, J. Comput. Aided Mol. Des. 22 (2008) 925–933.
[19] J. Deng, K.W. Lee, T. Sanchez, M. Cui, N. Neamati, J.M. Briggs, Dynamic receptor-based pharmacophore model development and its application in designing novel HIV-1 integrase inhibitors, J. Med. Chem. 48 (2005) 1496–1505.
[20] H.J. Bohm, The computer program LUDI: a new method for the de novo design of enzyme inhibitors, J. Comput. Aided Mol. Des. 6 (1992) 61–78.
[21] H.J. Bohm, LUDI: rule-based automatic design of new substituents for enzyme inhibitor leads, J. Comput. Aided Mol. Des. 6 (1992) 593–606.
[22] D. Moras, H. Gronemeyer, The nuclear receptor ligand-binding domain: structure and function, Curr. Opin. Cell Biol. 10 (1998) 384–391.
[23] D.S. 3.0, Accelrys Inc., San Diego, CA, USA.
[24] E.M. Krovat, K.H. Fruhwirth, T. Langer, Pharmacophore identification, in silico screening, and virtual library design for inhibitors of the human factor Xa, J. Chem. Inform. Model. 45 (2005) 146–159.
[25] N. Belkina, M. Lisurek, A. Ivanov, R. Bernhardt, Modelling of three-dimensional structures of cytochromes P450 11B1 and 11B2, J. Inorg. Biochem. 87 (2001) 197–207.
[26] F. Chan, J. Zhang, L. Cheng, D.N. Shapiro, A. Winoto, Identification of human and mouse p19, a novel CDK4 and CDK6 inhibitor with homology to p16ink4, Mol. Cell. Biol. 15 (1995) 2682.
[27] X. Chen, Y. Lin, M. Liu, M.K. Gilson, The binding database: data management and interface design, Bioinformatics 18 (2002) 130.
[28] A. Smellie, S.D. Kahn, S.L. Teig, Analysis of conformational coverage. 2. Applications of conformational models, J. Chem. Inf. Comput. Sci. 35 (1995) 295–304.
[29] A. Smellie, S.L. Teig, P. Towbin, Poling: promoting conformational variation, J. Comput. Chem. 16 (1995) 171–187.
[30] A. Smellie, S.D. Kahn, S.L. Teig, Analysis of conformational coverage. 1. Validation and estimation of coverage, J. Chem. Inf. Comput. Sci. 35 (1995) 285–294.
[31] I.V. Tetko, The WWW as a tool to obtain molecular parameters, Mini Rev. Med. Chem. 3 (2003) 809–820.
[32] P. Ertl, B. Rohde, P. Selzer, Fast calculation of molecular polar surface area as a sum of fragment-based contributions and its application to the prediction of drug transport properties, J. Med. Chem. 43 (2000) 3714–3717.
[33] C.A. Lipinski, F. Lombardo, B.W. Dominy, P.J. Feeney, Experimental and computational approaches to estimate solubility and permeability in drug discovery and development settings, Adv. Drug Deliver. Rev. 23 (1997) 3–25.
[34] D.F. Veber, S.R. Johnson, H.Y. Cheng, B.R. Smith, K.W. Ward, K.D. Kopple, Molecular properties that influence the oral bioavailability of drug candidates, J. Med. Chem. 45 (2002) 2615–2623.
[35] M.L. Verdonk, J.C. Cole, M.J. Hartshorn, C.W. Murray, R.D. Taylor, Improved protein–ligand docking using GOLD, Proteins: Struct. Funct. Bioinform. 52 (2003) 609–623.
[36] L.K. Worf, New software and websites for the chemical enterprise, Chem. Eng. News 87 (2009) 32.
[37] E. Lindahl, B. Hess, D. van der Spoel, GROMACS 3.0: a package for molecular simulation and trajectory analysis, J. Mol. Model. 7 (2001) 306–317.
[38] X.M. Chen, T. Lu, S. Lu, H.F. Li, H.L. Yuan, T. Ran, H.C. Liu, Y.D. Chen, Structure-based and shape-complemented pharmacophore modeling for the discovery of novel checkpoint kinase 1 inhibitors, J. Mol. Model. 16 (2010) 1195–1204.
[39] B.R. Henke, Peroxisome proliferator-activated receptor α/γ ducal agonists for the treatment of type 2 diabetes, J. Med. Chem. 47 (2004) 4118–4127.